

Tau neutrino as a probe of nonstandard interactions via charged Higgs and W' contribution

AHMED RASHED¹

*Department of Physics and Astronomy
University of Mississippi, Lewis Hall, University, MS, 38677, USA*

*Department of Physics, Faculty of Science
Ain Shams University, Cairo, 11566, Egypt*

We discuss the impact of the presence of a charged Higgs and a W' gauge boson on the tau-neutrino nucleon scattering $\nu_\tau + N \rightarrow \tau^- + X$ and $\bar{\nu}_\tau + N \rightarrow \tau^+ + X$. We show the effect of the new physics on the three subprocesses quasielastic, Δ -resonance, and deep inelastic scattering. The measurement of the atmospheric and reactor mixing angles θ_{23} and θ_{13} , respectively, relies on the standard model cross section of the above processes if they have been measured in the appearance channels $\nu_\mu \rightarrow \nu_\tau$ and $\bar{\nu}_e \rightarrow \bar{\nu}_\tau$ ($\nu_e \rightarrow \nu_\tau$), respectively. Consideration of the new physics contributions to those reactions modifies the measured mixing angles, assuming the standard model cross section. We include form factor effects in the new physics calculations and find the deviations of the mixing angles which can be significant and can depend on the energy of the neutrino.

PRESENTED AT

DPF 2013

The Meeting of the American Physical Society
Division of Particles and Fields
Santa Cruz, California, August 13–17, 2013

¹This work supported in part by the National Science Foundation under Grant No. NSF PHY-1068052.

The effects of nonstandard interaction (NSI) on neutrino oscillation have been widely studied [1]. It has been established that NSI cannot be an explanation for the standard oscillation phenomena, but it may be present as a subleading effect. General bounds on the NSI parameters have been discussed in the literatures [2]. The NSI impact has been studied on different themes in neutrino phenomenology [3]. Often in the analysis of NSI, hadronization effects of the quarks via form factors are not included. In Ref. [4, 5], the results show that the form factors play an important role in the energy dependence of the NSI effects. Many NSI involve flavor changing neutral current or charged current lepton flavor violating processes. Here we consider charged current interactions involving contributions from a charged Higgs and a W' gauge boson. In neutrino experiments, to measure the mixing angle the neutrino-nucleus interaction is assumed to be SM-like. If there is a charged Higgs or a W' contribution to this interaction, then there will be an error in the extracted mixing angle. We will calculate the error in the extracted mixing angle. Constraints on the new couplings come from the hadronic τ decays. We will consider constraints from the decays $\tau^- \rightarrow \pi^- \nu_\tau$ and $\tau^- \rightarrow \rho^- \nu_\tau$ [4, 5].

There are several reasons to consider NSI involving the (ν_τ, τ) sector. First, the third generation may be more sensitive to new physics effects because of their larger masses. As an example, in certain versions of the two Higgs doublet models (2HDM) the couplings of the new Higgs bosons are proportional to the masses, and so new physics effects are more pronounced for the third generation. Second, the constraints on NP involving the third generation leptons are somewhat weaker, allowing for larger new physics effects. Interestingly, the branching ratio of B decays to τ final states shows some tension with the SM predictions [6, 7] and this could indicate NP, possibly in the scalar or gauge boson sector [8]. Some examples of work that deals with NSI at the detector, though not necessarily involving the third family leptons, can be found in Refs. [9, 10].

The process $\nu_\tau + N \rightarrow \tau^- + X$ will impact the measurement of the oscillation probability for the $\nu_\mu \rightarrow \nu_\tau$ transition and hence the extraction of the mixing angle θ_{23} . The measurement of the atmospheric mixing angle θ_{23} relies on the following relationship [11]:

$$N(\nu_\tau) = P(\nu_\mu \rightarrow \nu_\tau) \times \Phi(\nu_\mu) \times \sigma_{\text{SM}}(\nu_\tau), \quad (1)$$

where $N(\nu_\tau)$ is the number of observed events, $\Phi(\nu_\mu)$ is the flux of muon neutrinos at the detector, $\sigma^{\text{SM}}(\nu_\tau)$ is the total cross section of tau neutrino interactions with nucleons in the SM at the detector, and $P(\nu_\mu \rightarrow \nu_\tau)$ is the probability for the flavor transition $\nu_\mu \rightarrow \nu_\tau$. This probability is a function of $(E, L, \Delta m_{ij}^2, \theta_{ij})$ with $i, j = 1, 2, 3$, where Δm_{ij}^2 is the squared-mass difference, θ_{ij} is the mixing angle, E is the energy of neutrinos, and L is the distance traveled by neutrinos. The dominant term of the probability is

$$P(\nu_\mu \rightarrow \nu_\tau) \approx \sin^2 2\theta_{23} \cos^4 \theta_{13} \sin^2(\Delta m_{23}^2 L/4E). \quad (2)$$

In the presence of NP, Eq. 1 is modified as

$$N(\nu_\tau) = P(\nu_\mu \rightarrow \nu_\tau) \times \Phi(\nu_\mu) \times \sigma_{\text{tot}}(\nu_\tau), \quad (3)$$

with $\sigma_{\text{tot}}(\nu_\tau) = \sigma_{\text{SM}}(\nu_\tau) + \sigma_{\text{NP}}(\nu_\tau)$, where $\sigma_{\text{NP}}(\nu_\tau)$ refers to the additional terms of the SM contribution towards the total cross section. Hence, $\sigma_{\text{NP}}(\nu_\tau)$ includes contributions

from both the SM and NP interference amplitudes, and the pure NP amplitude. From Eqs. (1, 3), assuming θ_{13} to be small,*

$$\sin^2 2(\theta_{23}) = \sin^2 2(\theta_{23})_{SM} \frac{1}{1 + r_{23}}, \quad (4)$$

where $\theta_{23} = (\theta_{23})_{SM} + \delta_{23}$ is the actual atmospheric mixing angle, whereas $(\theta_{23})_{SM}$ is the extracted mixing angle assuming the SM ν_τ scattering cross section. Assuming negligible new physics effects in the $\mu - N$ interaction, the actual mixing angle θ_{23} is the same as the mixing angle extracted from the survival probability $P(\nu_\mu \rightarrow \nu_\mu)$ measurement. We will take the best-fit value for the mixing angle to be given by $\theta_{23} = 42.8^\circ$ [12]. In other words, the presence of new physics in a ν_τ -nucleon scattering will result in the mixing angle, extracted from a ν_τ appearance experiment, being different than the mixing angle from ν_μ survival probability measurements. The relationship between the ratio of the NP contribution to the SM cross section $r_{23} = \sigma_{NP}(\nu_\tau)/\sigma_{SM}(\nu_\tau)$ and δ_{23} can be expressed in a model-independent form as

$$r_{23} = \left[\frac{\sin 2(\theta_{23})_{SM}}{\sin 2((\theta_{23})_{SM} + \delta_{23})} \right]^2 - 1. \quad (5)$$

The reactor mixing angle θ_{13} can be determined from the oscillation probability of the appearance channel $\bar{\nu}_e \rightarrow \bar{\nu}_\tau$ ($\nu_e \rightarrow \nu_\tau$). In this case the effect of NP contributions to the process $\bar{\nu}_\tau + N \rightarrow \tau^+ + X$ ($\nu_\tau + N \rightarrow \tau^- + X$) is pertinent. The best-fit value for the mixing angle to be given by $\theta_{13} = 9.1^\circ$ [13]. Many neutrino mixing models have expected non-zero value for θ_{13} [14]. The relationship, e.g., used in measuring θ_{13} will be given as

$$N(\bar{\nu}_\tau) = P(\bar{\nu}_e \rightarrow \bar{\nu}_\tau) \times \Phi(\bar{\nu}_e) \times \sigma_{\text{tot}}(\bar{\nu}_\tau), \quad (6)$$

where [15, 16, 17]

$$P(\bar{\nu}_e \rightarrow \bar{\nu}_\tau) \approx \sin^2 2\theta_{13} \cos^2 \theta_{23} \sin^2(\Delta m_{13}^2 L/4E). \quad (7)$$

Thus the relationship between the ratio of the NP contribution to the SM cross section $r_{13} = \sigma_{NP}(\bar{\nu}_\tau)/\sigma_{SM}(\bar{\nu}_\tau)$ and δ_{13} can be obtained in a model-independent form as

$$r_{13} = \left[\frac{\sin 2(\theta_{13})_{SM}}{\sin 2((\theta_{13})_{SM} + \delta_{13})} \right]^2 - 1. \quad (8)$$

In Fig. 1 we show the correlation between $r_{23(13)}\%$ and $\delta_{23(13)} [\text{Deg}]$. One can see that $\delta_{23} \sim -5^\circ$ requires $r_{23} \sim 5\%$. But $\delta_{13} \sim -1^\circ$ requires $r_{13} \sim 25\%$.

The coupling of charged Higgs boson (H^\pm) interactions to a SM fermion in the 2HDM II is [18]

$$\mathcal{L} = \frac{g}{\sqrt{2}M_W} \sum_{ij} \left[m_{u_i} \cot \beta \bar{u}_i V_{ij} P_{L,R} d_j + m_{d_j} \tan \beta \bar{u}_i V_{ij} P_{R,L} d_j + m_{l_j} \tan \beta \bar{\nu}_i P_{R,L} l_j \right] H^\pm, \quad (9)$$

*The presence of NP impacts the extraction of the combination $\sin^2 2\theta_{23} \cos^4 \theta_{13}$. The NP changes the extracted value of θ_{23} as well as θ_{13} . But we fix the value of θ_{13} as an input at this point.

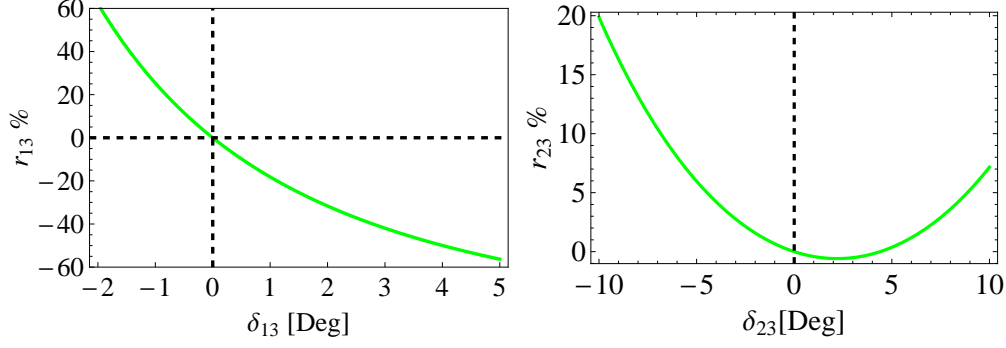


Figure 1: Correlation plot for $r_{23} = \sigma_{NP}(\nu_\tau)/\sigma_{SM}(\nu_\tau)\%$ versus $\delta_{23}[Deg]$, and $r_{13} = \sigma_{NP}(\bar{\nu}_\tau)/\sigma_{SM}(\bar{\nu}_\tau)\%$ versus $\delta_{13}[Deg]$.

where $P_{L,R} = (1 \mp \gamma^5)/2$, and $\tan \beta$ is the ratio between the two vacuum expectation values (vev's) of the two Higgs doublets, and

$$\begin{aligned} g_S^{u_i d_j} &= \left(\frac{m_{d_j} \tan \beta + m_{u_i} \cot \beta}{M_W} \right), \\ g_P^{u_i d_j} &= \left(\frac{m_{d_j} \tan \beta - m_{u_i} \cot \beta}{M_W} \right), \\ g_S^{\nu_i l_j} &= g_P^{\nu_i l_j} = \frac{m_{l_j} \tan \beta}{M_W}. \end{aligned} \quad (10)$$

The lowest dimension effective Lagrangian of W' interactions to the SM fermions has the form

$$\mathcal{L} = \frac{g}{\sqrt{2}} V_{f'f} \bar{f}' \gamma^\mu (g_L^{f'f} P_L + g_R^{f'f} P_R) f W'_\mu + h.c., \quad (11)$$

where f' and f refer to the fermions and $g_{L,R}^{f'f}$ are the left- and the right-handed couplings of the W' . For a SM-like W' boson, $g_L^{f'f} = 1$ and $g_R^{f'f} = 0$. We will assume $g_{L,R}^{f'f}$ to be real.

In Figs. (2, 3), we show the deviation of the mixing angles θ_{23} and θ_{13} due to the contribution of the charged Higgs to the tau-neutrino cross section. The deviations δ_{23} and δ_{13} are negative, as there is no interference with the SM; hence, the cross section for $\nu_\tau + N \rightarrow \tau^- + X$ and $\bar{\nu}_\tau + N \rightarrow \tau^+ + X$ are always larger than the SM cross section. This means that, if the actual θ_{23} is close to maximal, then experiments should measure θ_{23} larger than the maximal value in the presence of a charged Higgs contribution. In the Δ -RES and DIS cases, their effect has been introduced with considering the flux of the incoming muon-neutrinos and integrating over the possible atmospheric neutrino energy. In Figs. (4, 5, 6), we show the deviation δ_{23} with including the flux effect in the Δ -RES and DIS cases.

We calculate the number of events in the DIS W' model. We compare between the number of events of the atmospheric neutrinos in the SM $N_{SM} = 30.66 \pm 3.37$ and in the NP $N_{NSI} = 41.49$ for $M_{W'} = 200$ GeV. This shows that the N_{NSI} falls beyond the uncertainty of N_{SM} and so the NSI is potentially detectable.

References

- [1] See for example: L. Wolfenstein, Phys. Rev. D **17**, 2369 (1978).
- [2] See for example: J. Abdallah *et al.* [DELPHI Collaboration], Eur. Phys. J. C **38**, 395 (2005) [arXiv:hep-ex/0406019]. C. Biggio, M. Blennow and E. Fernandez-Martinez, JHEP **0908**, 090 (2009) [arXiv:0907.0097 [hep-ph]].
- [3] See for example: S. Bergmann, Y. Grossman and D. M. Pierce, Phys. Rev. D **61**, 053005 (2000) [hep-ph/9909390].
- [4] A. Rashed, M. Duraismy and A. Datta, Phys. Rev. D **87**, 013002 (2013) [arXiv:1204.2023 [hep-ph]].
- [5] A. Rashed, P. Sharma and A. Datta, arXiv:1303.4332 [hep-ph]. Accepted for publication in Nuclear Physics B.
- [6] K. Ikado *et al.*, Phys. Rev. Lett. **97**, 251802 (2006) [arXiv:hep-ex/0604018].
- [7] J. P. Lees *et al.* [BaBar Collaboration], Phys. Rev. Lett. **109**, 101802 (2012) [arXiv:1205.5442 [hep-ex]].
- [8] A. Datta, M. Duraismy and D. Ghosh, Phys. Rev. D **86**, 034027 (2012) [arXiv:1206.3760 [hep-ph]].
- [9] M. C. Gonzalez-Garcia, Y. Grossman, A. Gusso and Y. Nir, Phys. Rev. D **64**, 096006 (2001) [hep-ph/0105159].
- [10] C. Biggio, M. Blennow and E. Fernandez-Martinez, JHEP **0908**, 090 (2009) [arXiv:0907.0097 [hep-ph]].
- [11] T. Teshima and T. Sakai, Analysis of atmospheric neutrino oscillations in three flavor neutrinos, Phys. Rev. D **62**, 113010 (2000) [hep-ph/0003038].
- [12] M. C. Gonzalez-Garcia, M. Maltoni and J. Salvado, JHEP **1004**, 056 (2010) [arXiv:1001.4524 [hep-ph]].
- [13] D. V. Forero, M. Tortola and J. W. F. Valle, arXiv:1205.4018 [hep-ph].
- [14] E. Ma, A. Natale and A. Rashed, Int. J. Mod. Phys. A **27**, 1250134 (2012) [arXiv:1206.1570 [hep-ph]]. A. Rashed, Nucl. Phys. B **874**, 679 (2013) [arXiv:1111.3072 [hep-ph]]. A. Rashed and A. Datta, Phys. Rev. D **85**, 035019 (2012) [arXiv:1109.2320 [hep-ph]]. S. Bhattacharya, E. Ma, A. Natale and A. Rashed, Phys. Rev. D **87**, 097301 (2013) [arXiv:1302.6266 [hep-ph]].
- [15] A. Donini, D. Meloni and P. Migliozzi, Nucl. Phys. B **646**, 321 (2002) [hep-ph/0206034].
- [16] A. Upadhyay and M. Batra, arXiv:1112.0445 [hep-ph].

- [17] P. Huber, M. Lindner, M. Rolinec and W. Winter, Phys. Rev. D **74**, 073003 (2006) [hep-ph/0606119].
- [18] See, e.g., R. A. Diaz, hep-ph/0212237, O. Deschamps, S. Descotes-Genon, S. Monteil, V. Niess, S. T’Jampens and V. Tisserand, Phys. Rev. D **82**, 073012 (2010) [arXiv:0907.5135 [hep-ph]], G. C. Branco, P. M. Ferreira, L. Lavoura, M. N. Rebelo, M. Sher and J. P. Silva, arXiv:1106.0034 [hep-ph].
- [19] M. Honda, T. Kajita, K. Kasahara and S. Midorikawa, Phys. Rev. D **83**, 123001 (2011) [arXiv:1102.2688 [astro-ph.HE]].

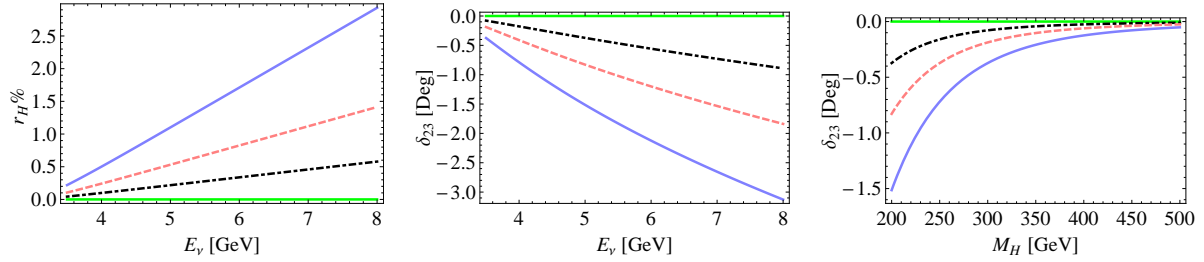


Figure 2: Quasi-elastic (H^+): Variation of $r_H^{23}\%$ with E_ν and variation of δ_{23} with M_H and E_ν . The green line corresponds to the SM prediction. The black (dotdashed), pink (dashed), and blue (solid) lines correspond to $\tan\beta = 40, 50, 60$. The right figure is evaluated at $E_\nu = 5$ GeV, while the left figures are evaluated at $M_H = 200$ GeV. Here, we use the best-fit value $\theta_{23} = 42.8^\circ$ [12].

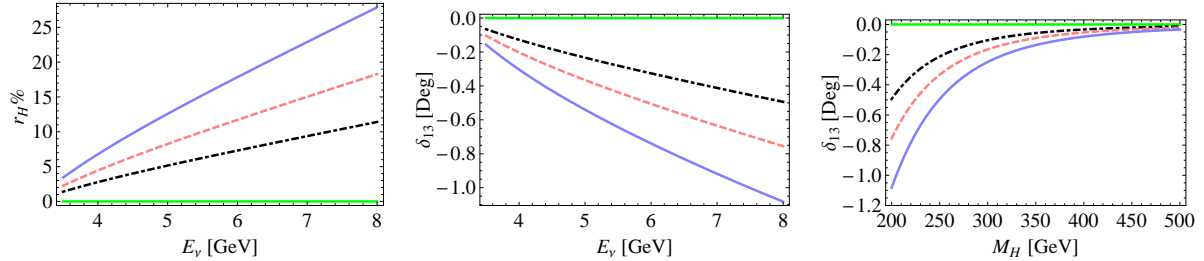


Figure 3: Quasi-elastic (H^+): Variation of $r_H^{13}\%$ with E_ν and the variation of δ_{13} with M_H and E_ν . The green line corresponds to the SM prediction. The black (dotdashed), pink (dashed), and blue (solid) lines correspond to $\tan\beta = 80, 90, 100$. The right figure is evaluated at $E_\nu = 8$ GeV, while the left figures are evaluated at $M_H = 200$ GeV. Here, we use the inverted hierarchy value $\theta_{13} = 9.1^\circ$ [13].

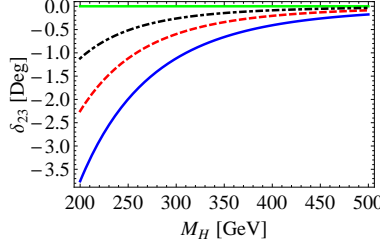


Figure 4: Resonance (H): The figures illustrate variation of δ_{23} with M_H . The green line corresponds to the SM prediction. The black (dotdashed), red (dashed), and blue (solid) lines correspond to $\tan \beta = 40, 50, 60$. Here, we use the best-fit value $\theta_{23} = 42.8^\circ$ [12]. We take into account the atmospheric neutrino flux for Kamioka where the Super-Kamiokande experiment locates [19].

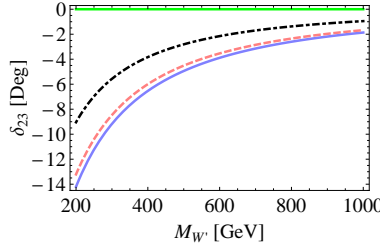


Figure 5: Resonance (W'): The figure illustrates the deviation δ_{23} with the W' mass $M_{W'}$ when both left and right-handed W' couplings are present. The lines show predictions for some representative values of the W' couplings ($g_L^{\tau\nu\tau}, g_L^{ud}, g_R^{ud}$). The green line (solid, upper) corresponds to the SM prediction. The blue line (solid, lower) corresponds to $(-0.94, -1.13, -0.85)$. Here, we use the best-fit value $\theta_{23} = 42.8^\circ$ [12]. We take into account the atmospheric neutrino flux for Kamioka where the Super-Kamiokande experiment locates [19].

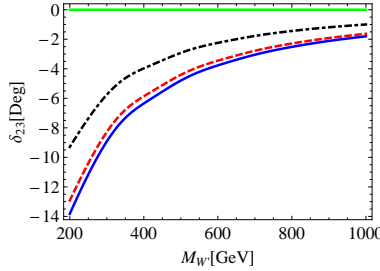


Figure 6: DIS (W'): The figure illustrates the deviation δ_{23} with the W' mass $M_{W'}$ when both left and right-handed W' couplings are present. The lines show predictions for some representative values of the W' couplings ($g_L^{\tau\nu\tau}, g_L^{ud}, g_R^{ud}$). The green line (solid, upper) corresponds to the SM prediction. The blue line (solid, lower) corresponds to $(-0.94, -1.13, -0.85)$. Here, we use the best-fit value $\theta_{23} = 42.8^\circ$ [12]. We take into account the atmospheric neutrino flux for Kamioka where the Super-Kamiokande experiment locates [19].